DOI: 10.1002/chem.201000218

Selective Monoacylation of Ferrocene with Bulky Acylating Agents over Mesoporous Sieve AlKIT-5

Dana Procházková,[a] Martina Bejblová,[a] Josef Vlk,[a] Ajayan Vinu,[b] Petr Štěpnička,[c] and Jiří Čejka*[a]

Abstract: Ferrocene acylation with bulky acylating agents (1-adamantoyl, benzoyl, 2-chlorobenzoyl, and cinnamoyl chlorides; and benzoic anhydride) catalyzed by AlKIT-5 mesoporous catalysts was investigated. AlKIT-5 catalysts with varying ratios of Si/Al were synthesized using tetraethoxysilane and aluminum isopropoxide as the structural building blocks and Pluronic F127 as a template under acidic conditions and were characterized in detail by X-ray powder diffraction, magic-angle spinning (MAS) NMR spectroscopy, sorption of nitrogen, energy-dispersive X-ray spectroscopy (EDS), SEM, TEM, and FTIR with pyridine as a probe molecule. The catalytic activity of the prepared AlKIT-5 catalysts in ferrocene acylation was shown to depend on the type of the acylating agent, thus likely reflecting the strength of interactions between the acyl source, the product, and the solid catalysts when the acylation reaction was carried out at 100 °C. In all reactions, the AlKIT-5 catalysts afforded exclusively the monoacylated products (100 % selectivity) most likely due to deactivation of the second cyclopentadiene ring by attachment of the first acyl group, steric reasons, and some competitive interactions of the monoacylferrocenes with the catalysts. The prepared AlKIT-5 catalysts could be regenerated without any significant loss of the ferrocene conversion.

Keywords: acylation · aluminum · ferrocene · mesoporous materials · silicon

Introduction

Friedel–Crafts acylations represent an important synthetic method that leads to aromatic ketones, which are highly valued intermediates in the synthesis of pharmaceuticals, fragrances, flavors, dyes, and agrochemicals.[1] For many decades, conventional catalysts like $AlCl_3$, $FeCl_3$, HF, and H_2SO_4 were used to mediate these reactions despite their numerous disadvantages including environmental issues, corrosion, and the necessity to use them in over-stoichiometric amounts.[2,3] Recently, zeolites and mesoporous molecular sieves emerged as promising catalysts for Friedel–Crafts acylations; they show both high activities and selectivites in the reactions that involve various aromatic hydrocarbons and olefins.[4–10] With respect to that, mesoporous materials that possess three-dimensional cage-type pore structures such as SBA-1, SBA-16, and KIT-5 are nowadays considered more promising as they are more resistant to pore blocking, they allow for a faster diffusion of the reactants, and they provide more adsorption sites, which are more accessible through the three-dimensional porous structure.[11]

Mesoporous molecular sieves have received considerable attention owing to their narrow pore-size distributions, high surface areas, and large pore volumes.[12–16] Among the materials mentioned above, KIT-5 is particularly interesting as it possesses a highly ordered three-dimensional mesoporous structure with cubic *Fm3m* close-packed symmetry, a large surface area, pores with tunable diameter, a large specific pore volume, and large cages.[17] Such properties make this material attractive for applications that range from adsorption of small molecules to the fabrication of mesoporous carbon with a cage-type porous structure.[18,19] The catalytic application of pure silica KIT-5 remains still to be explored,

[a] Dr. D. Procházková, Dr. M. Bejblová, J. Vlk, Prof. J. Čejka
J. Heyrovský Institute of Physical Chemistry, v.v.i.
Academy of Sciences of the Czech Republic
Dolejškova 3, 182 23 Prague (Czech Republic)
Fax: (+420) 28658-2307
E-mail: jiri.cejka@jh-inst.cas.cz

[b] Prof. A. Vinu
International Center for Materials Nanoarchitectonics
World Premier International Research Center
National Institute for Materials Science
1-1 Namiki, Tsukuba 305-0044 (Japan)

[c] Prof. P. Štěpnička
Department of Inorganic Chemistry, Faculty of Science
Charles University in Prague
Hlavova 2030, 12840 Prague 2, Czech Republic

probably due to the low acidity and poor ion-exchange capability of this material. Very recently, Vinu and co-workers discovered an alternative direct synthetic route to Al-substituted KIT-5 materials with high aluminum loading (i.e., with n_{Al}/n_{Si} ratios up to 0.10). The resulting AlKIT-5 catalysts were studied in the acylation of veratrole with acetic anhydride and the results were compared with those obtained over zeolites Beta, H-ZSM-5, HY, and Mordenite. It was found that the conversion of acetic anhydride increased with increasing content of Al in the (Al)KIT-5 material (n_{Si}/n_{Al} ratios are given in brackets): (Al)KIT-5 (71) 39% < (Al)KIT-5 (44) 50% < (Al)KIT-5 (28) 63% < (Al)KIT-5 (10) 69%. For zeolites, on the other hand, the following order of acetic anhydride conversions was established: H-Y (13.5) 63% > H-Beta (30) 53% > H-Mordenite (20) 12% > H-ZSM-5 (60) 9%.[20,21]

Whereas aromatic hydrocarbons and, less frequently, olefins are typical substrates for acylation reactions, acylation of ferrocene is extremely rare over zeolite catalysts.[22] This is rather surprising when one considers the importance of various ferrocene derivatives and their interesting applications as intermediates in the production of functional materials such as metal-containing polymers, charge-transfer complexes, chiral ligands, and biologically active compounds.[23] Indeed, ferrocene is highly active in acylation reactions. However, the preparation of acylferrocenes should avoid oxidizing conditions because of an easy oxidation of ferrocenes to the corresponding ferrocenium salts. Furthermore, since both coordinated cyclopentadienyls in ferrocene react rather independently in Friedel–Crafts reactions, it is difficult to control the reaction course in terms of selectivity (mono- vs. 1,1′-diacylation; Scheme 1). Thus, whereas the

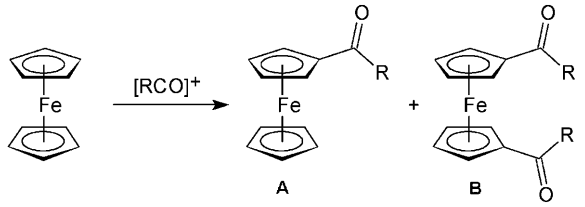

Scheme 1. Acylation of ferrocene.

preparation of 1,1′-diacylferrocenes (**B**) is usually achieved upon using an excess amount of an acylating agent, the preparation of monoacylferrocenes (**A**) requires careful control of the reaction conditions (solvent, amounts of reagents, temperature, and so on) and tedious isolation[24] or, alternatively, the use of nonconventional catalysts.[25]

The objective of this contribution was to study the application of novel AlKIT-5 mesoporous sieve catalysts in the acylation of ferrocene with bulky acylating agents. The effect of the acylating agent, reaction conditions, and catalyst composition (Si/Al ratio) on the conversion and selectivity in ferrocene acylations with 1-adamantoyl chloride, benzoyl chloride, benzoic anhydride, 2-chlorobenzoyl chloride, and cinnamoyl chloride was investigated in a detail (Scheme 2).

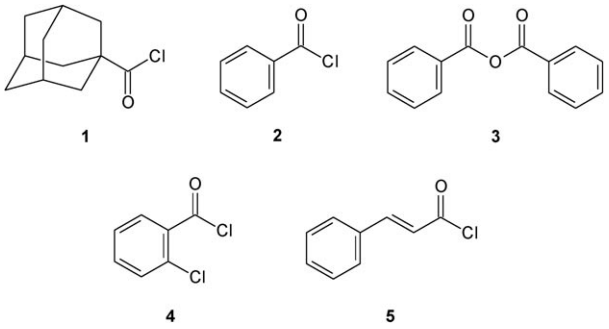

Scheme 2. Acylating agents used throughout this study: 1-adamantoyl chloride (**1**), benzoyl chloride (**2**), benzoic anhydride (**3**), 2-chlorobenzoyl chloride (**4**), and cinnamoyl chloride (**5**).

Experimental Section

Chemicals: All acylating agents were purchased from commercial suppliers (1-adamantoyl chloride from Acros, all other from Sigma–Aldrich) and were used as received.

Synthesis of the catalysts: AlKIT-5 materials with different n_{Si}/n_{Al} ratios were synthesized using the commercial nonionic Pluronic F127 surfactant (BASF) in an acidic medium. In a typical synthesis, a mixture of Pluronic F127 (5.0 g), aqueous HCl (3.0 g of 35 wt% solution), and distilled water (240 g) was stirred for 2–3 h at 45°C. Tetraethoxysilane (24.0 g) and the required amount of aluminum isopropoxide were added, and the reaction mixture was stirred at 45°C for 24 h and then hydrothermally treated under static conditions at 100°C for 24 h. The resulting solid was filtered off, dried at 100°C (without washing), and finally calcined at 540°C for 10 h. The composition of the reaction mixture expressed as SiO_2/Al_2O_3/F127/HCl/H_2O in terms of molar ratio was 1.0:0.041–0.071:0.0035:0.25:116.6.[20,21] The samples are denoted as AlKIT-5 (x), in which x stands for the n_{Si}/n_{Al} molar ratio in the final product.

Characterization of the mesoporous materials: The powder X-ray diffraction patterns of AlKIT-5 samples were collected using a Rigaku diffractometer and $Cu_{K\alpha}$ ($\lambda = 0.154$ nm) radiation. The diffractograms were recorded in the 2θ range of 0.7 to 10° (2θ step 0.01°, integration time 6 s). Nitrogen adsorption isotherms were measured at −196°C using a Quantachrome Autosorb 1 sorption analyzer. Prior to analysis, the samples were degassed for 3 h at 250°C under vacuum (10^{-6} Pa) in the degassing port of the analyzer. The specific surface area and the pore-size distribution were obtained from the adsorption branch of the isotherm using the BET equation and the Barrett–Joyner–Halenda (BJH) method, respectively.[26]

The morphology of the mesoporous materials was studied using a Hitachi S-4800 HR-FESEM with an acceleration voltage of 10 kV, whereas the elemental mapping and EDS analyses were obtained using the same instrument with an acceleration voltage of 30 kV. The HRTEM images were obtained using a JEOL JEM-2100F instrument. The accelerating voltage of the electron beam was 200 kV. ^{27}Al MAS NMR spectra were recorded using a Bruker MSL500 spectrometer (operating frequency 130.319 MHz) with 4 mm diameter zirconia rotors spun at a rotation frequency of 12 kHz. The elemental composition of the materials was determined by inductively coupled plasma atomic emission spectrometry (ICP-AES).

The concentration of Lewis (L) and Brønsted (B) acid sites was determined after adsorption of pyridine and FTIR spectroscopic analysis. The

mesoporous catalysts were pressed into self-supporting wafers with a density of 8–12 mg cm^{-2} and activated in situ under vacuum at 450 °C. Before the adsorption, pyridine was degassed by repeated freeze–pump–thaw cycles. Adsorption then proceeded at 150 °C and partial pressure of 950 Pa for 30 min, followed by desorption for 20 min. To evaluate the strength of the acid sites, further desorption steps were carried out at 250, 350, and 450 °C. All FTIR spectra were recorded using a Nicolet Protégé spectrometer (resolution 2 cm^{-1}, 128 scans for a single spectrum) and were normalized on wafer thickness of 10 mg cm^{-2}. Concentrations of Brønsted and Lewis acid sites were determined from the integral intensities of adsorption bands at 1545 cm^{-1} (Brønsted acid sites) and 1450 cm^{-1} (Lewis acid sites) using the published extinction coefficients ($\varepsilon_B = (1.67 \pm 0.1)$ cm μmol^{-1}, $\varepsilon_L = (2.22 \pm 0.1)$ cm μmol^{-1}).[27]

Catalytic tests: Acylation reactions were investigated using a Heidolph Synthesis 1 (system of 16 parallel reactors) in a liquid phase under atmospheric pressure. Prior to catalytic experiments, each catalyst was activated at 450 °C for 90 min and then cooled in a dessicator.

In a typical experiment, ferrocene (0.6 g, Fluka), decahydronaphthalene (8 mL, Fluka, solvent), dodecane (0.2 g, Aldrich, internal standard), and activated catalyst (0.6 g) were heated at 100 °C. Then the acylation agent was added to the reaction mixture at a ferrocene-to-acylating agent molar ratio that ranged from 1 to 6. Progress in the reaction was monitored on periodically withdrawn small aliquots, which were analyzed by gas chromatography (HP 6850 chromatograph equipped with FID detector and a high-resolution DB-5 capillary column: length 50 m, diameter 0.32 mm, phase thickness 10 μm).

Results and Discussion

Preparation and characterization of the catalysts: AlKIT-5 catalysts with varying ratios of Si/Al were obtained by hydrothermal treatment of an acidic synthesis gel that resulted through the addition of aqueous HCl to a mixture of tetraethoxysilane, aluminum isopropoxide (at different n_{Si}/n_{Al} ratios), and Pluronic F127 template polymer. Figure 1 shows the results of Si, O, and Al elemental mapping of the synthesized AlKIT-5 samples. The Si, O, and Al atoms appear to be uniformly distributed throughout the specimens. However, more dense Si and O elemental spots are observed compared to the spots due to Al. The density of the Al spots expectedly increases with increasing Al loading, thereby confirming that Al incorporation can be efficiently controlled by means of simply changing the amount of the Al source in the synthesis gel.

Powder XRD patterns of the prepared AlKIT-5 samples are presented in Figure S1 in the Supporting Information. All the materials show several diffraction lines at low θ angles, which can be indexed to the (111), (200), and (220) diffractions at the face-centered-cubic *Fm*3*m* lattice. Since the shape of the XRD pattern is almost identical to that of the pure siliceous KIT-5, one can assume that the structure of the AlKIT-5 is very similar to that of pure silica KIT-5 and, above all, remains unaffected even after incorporation of a relatively large amount of Al atoms in the parent siliceous framework. Upon increasing the Al content, the intensity of the (111) peak of the AlKIT-5 samples increases, whereas the peak shifts towards lower angles. This is probably because the unit cell of the materials expands upon incorporation of Al atoms into the parent KIT-5 structure. Generally, the increase in the unit cell dimensions upon the incorporation of Al atoms is related to the framework substitution in the silica walls, thus confirming that most of the Al atoms in AlKIT-5 are tetrahedrally surrounded with the Si atoms in the mesoporous walls.

High-resolution field-emission scanning electron microscopy (HR-FESEM) energy-dispersive X-ray spectroscopy (EDS) patterns (see Figure S2 in the Supporting Information) of the prepared materials display peaks that correspond to Al, Si, and O, thereby indicating the presence of aluminosilicate framework in the walls of the three-dimensional KIT-5 structure. The intensity of the Al peak increases with increased Al loading, and the n_{Si}/n_{Al} ratios obtained from the EDS patterns correlate well with the data obtained from ICP analysis. However, whereas the values of n_{Si}/n_{Al} ratios in the reaction mixture for three AlKIT-5 samples studied were 7, 10, and 12, the values determined for the synthesized materials were 10, 28, and 44, respectively, thereby indicating that not all aluminum from the reaction mixture was incorporated into the final products.

As indicated by HRSEM measurements (see representative micrograph in Figure 2A), the materials consist of aggregated spherical particles with a diameter of around 4–5 μm and a smoothed surface. High-resolution transmission

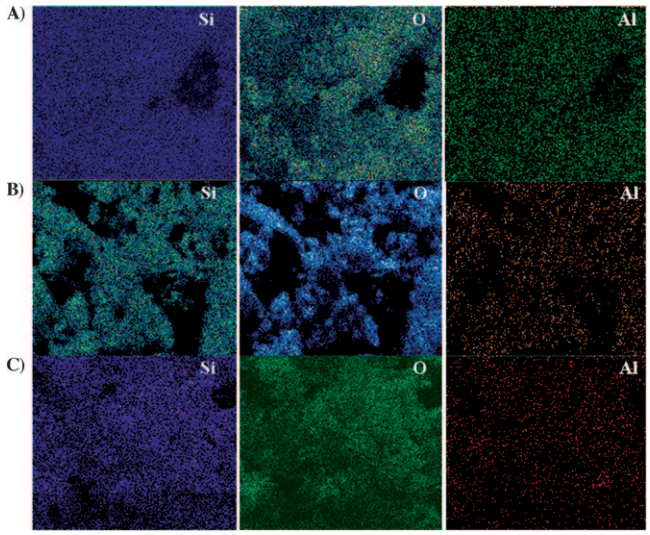

Figure 1. Elemental mapping of AlKIT-5 sample with different Al contents: A) AlKIT-5 (44), B) AlKIT-5 (28), and C) AlKIT-5 (10).

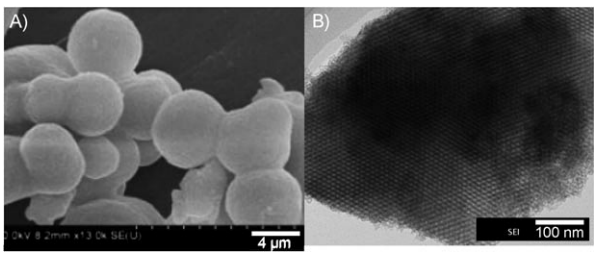

Figure 2. Representative A) HRSEM and B) HRTEM images of AlKIT-5 (44).

electron microscopy (HRTEM; Figure 2B) further revealed that the AlKIT-5 (44) possesses well-ordered three-dimensional mesostructure with uniform pores, which are arranged in regular intervals. These results confirm the retention of the mesostructural ordering even after the incorporation of Al atoms in the silica framework. Likewise, the nitrogen-adsorption isotherms (Figure 3) confirmed that all samples exhibit well-ordered mesoporous structure with excellent textural characteristics.

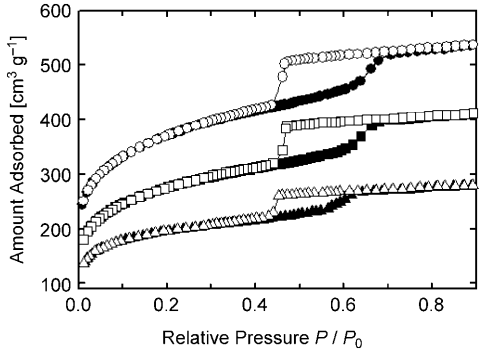

Figure 3. Nitrogen adsorption–desorption isotherms of AlKIT-5 samples with different Al contents: (▲) AlKIT-5 (44), (■) AlKIT-5 (28), and (●) AlKIT-5 (10) (closed symbols: adsorption; open symbols: desorption). The isotherms are mutually shifted by 50 $cm^3 g^{-1}$ along the y axis to avoid overlapping.

Textural parameters of the prepared AlKIT-5 samples are superior to those of the pure silica KIT-5.[20] The observed improvement in the textural properties (namely, an increase in the surface area, pore volume, and pore diameter) upon the incorporation of Al ions into the parent KIT-5 structure is a particularly interesting feature of the newly prepared materials. In particular, the specific surface area increases with a decrease in the n_{Si}/n_{Al} ratio (AlKIT-5 (44) 713 $m^2 g^{-1}$ > AlKIT-5 (28) 815 $m^2 g^{-1}$ > AlKIT-5 (10) 989 $m^2 g^{-1}$) and so does the pore volume and the pore diameter. The specific pore volume increases from 0.45 to 0.68 $cm^3 g^{-1}$ upon decreasing the n_{Si}/n_{Al} ratio from 44 to 10, whereas the pore diameter increases from 5.2 to 6.0 nm for the same samples, respectively. These results are in good agreement with the XRD measurements, which suggests that the structural ordering and the textural parameters are significantly improved upon incorporation of Al atoms into the KIT-5 silica structure.

The location and accessibility of aluminum, which are of critical importance for catalytic applications, were studied by a combination of ^{27}Al MAS NMR and FTIR spectroscopy with pyridine adsorption. The ^{27}Al MAS NMR spectra of AlKIT-5 samples with different Al contents (Figure 4) demonstrate the presence of two types of Al centers in the structure by exhibiting two resonances at around $\delta_{Al} = 53$ and 0 ppm. These signals can be attributed to Al atoms in a tetrahedral coordination with the silicate units and to the Al atoms with an octahedral coordination sphere, respectively. It is interesting to note that the intensity of the peak due to

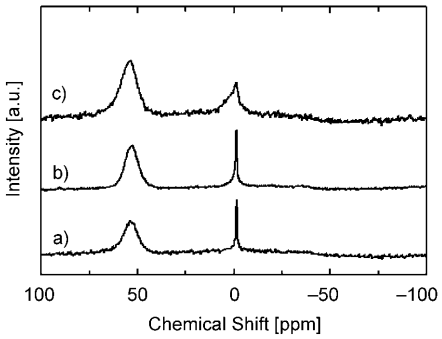

Figure 4. ^{27}Al MAS NMR spectra of AlKIT-5 samples with different Al contents: a) AlKIT-5 (44), b) AlKIT-5 (28), and c) AlKIT-5 (10). The resonances at around $\delta = 0$ and 55 ppm are attributable to octahedrally and tetrahedrally coordinated Al centers, respectively.

the tetrahedrally coordinated Al centers significantly increases upon increasing the Al content.

Although ^{27}Al MAS NMR spectroscopy provided the information about the coordination of Al ions, adsorption of pyridine followed by FTIR spectroscopy aided in determining the concentration and type of acid sites accessible by this probe molecule.[28] Pyridine was adsorbed at 150 °C for 20 min at a partial pressure of 900 Pa, followed by evacuation for 20 min at different temperatures (150, 250, 350, and 450 °C). The concentrations of Brønsted and Lewis acid sites were calculated from integral intensities of the bands characteristic for pyridine bound to Brønsted acid sites at 1546 cm^{-1} and for pyridine interacting with Lewis acid sites at 1456 cm^{-1}.[29]

The spectra in the hydroxyl group region (ν_{OH}) consist of a single absorption band, which is located at 3745 cm^{-1} in all three AlKIT-5 catalysts (see Figure 5 for the spectra of AlKIT-5 (28); FTIR spectra of other AlKIT-5 catalysts before and after adsorption are available in Figures S3 and

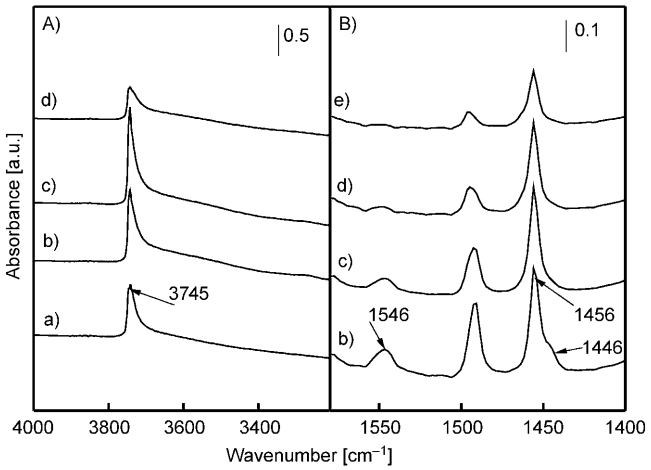

Figure 5. FTIR spectra of AlKIT-5 (28) in A) the region of ν_{OH} and B) vibrations of adsorbed pyridine recorded a) before pyridine adsorption, and after 20 min of pyridine desorption at b) 150, c) 250, d) 350, and e) 450 °C.

S4 in the Supporting information) and can be assigned to unassociated terminal silanol groups. Its intensity is only slightly affected by adsorption of pyridine at 150 °C, thereby resulting in the development of a band at 1446 cm^{-1}. The latter absorption band was not observed in the spectra of AlKIT-5 (10) whereas, in the spectra of AlKIT-5 (28) and AlKIT-5 (44), it disappears after desorption at 250 °C. This clearly evidences only a weak interaction between the pyridine molecules and the silanol groups in the prepared AlKIT-5 samples.

After pyridine adsorption, several new bands (in addition to a band at 1446 cm^{-1}) emerge in the IR spectra. The band at 1546 cm^{-1} is usually assigned to pyridinium ions formed by the interaction of pyridine with Brønsted acid sites. The estimated concentration of the Brønsted acid sites (Table 1) is rather low, which explains why no vibrations due to Si-OH-Al groups are detected in the ν_{OH} region. Furthermore, the band at 1456 cm^{-1} evidences the presence of pyridine interacting with strong Lewis acid sites (for concentrations, see figure and scheme captions). Substantial differences in the n_{Si}/n_{Al} ratios determined from the bulk analysis by ICP and calculated from FTIR spectra of adsorbed pyridine can be rationalized by the presence of Al atoms inside the AlKIT-5 walls where they cannot be accessed by the pyridine molecules.[28]

Table 1. Concentration of Lewis (L) and Brønsted (B) acid sites after pyridine desorption.

	AlKIT-5 (10)		AlKIT-5 (28)		AlKIT-5 (44)	
T [°C]	c_L [mmol g^{-1}]	c_B [mmol g^{-1}]	c_L [mmol g^{-1}]	c_B [mmol g^{-1}]	c_L [mmol g^{-1}]	c_B [mmol g^{-1}]
150	0.13	0.07	0.09	0.06	0.05	0.04
250	0.10	0.03	0.10	0.04	0.05	0.03
350	0.06	0.01	0.08	0.01	0.05	0.02
450	0.05	0	0.04	0.01	0.04	0.01

Following the changes in the amount of pyridine, which remains adsorbed on the AlKIT-5 samples after desorption performed at different temperatures, allowed us to gain some information on the acid strength of the individual acid sites. In the case of AlKIT-5 (10) and AlKIT-5 (28), the band at 1546 cm^{-1} attributed to Brønsted acid sites significantly diminished after pyridine desorption at 350 °C and completely disappeared after desorption at 450 °C. On the other hand, some pyridine (more than half of the original amount) remained adsorbed on the Lewis acid sites even after evacuation at 450 °C. For AlKIT-5 (44), the differences in concentrations of Lewis acid sites after desorption of pyridine at 150 and 450 °C are practically negligible, which stands in contrast to the behavior of AlKIT-5 catalysts that have higher aluminum concentrations. AlKIT-5 (44) also exhibits a higher stability of Brønsted acid sites at higher temperatures. As can be seen from Table 1, the acidic properties of all three AlKIT-5 catalysts after activation at 450 °C are very similar.

Acylation of ferrocene: Recently, we have shown that zeolites and mesoporous MCM-41 are active catalysts in ferrocene acylation with acetic anhydride or acetyl chloride.[22,30] As a continuation of our research, we now turned our attention to acylation of ferrocene with bulky acylating agents that provide useful synthetic intermediates[31] as well as products of interest for further applications.[32] In this study, we describe acylation reactions of ferrocene with 1-adamantoyl chloride (**1**), benzoyl chloride (**2**), cinnamoyl chloride (**5**), 2-chlorobenzoyl chloride (**4**), or benzoic anhydride (**3**; Scheme 2) over a new type of advanced catalyst: mesoporous AlKIT-5 sieves with different Si/Al ratios.

The progress in the acylation of ferrocene with 1-adamantoyl chloride over all AlKIT-5 catalysts studied is depicted in Figure 6. A substantial increase in ferrocene conversion is clearly seen during the first 30 min at 100 °C, whereas at prolonged reaction times the conversion tends to level off. Notably, the amounts of reacted ferrocene after 300 min of reaction time over all three catalysts are rather similar (AlKIT-5 (28): 50 %, AlKIT-5 (10): 48 %, AlKIT-5 (44): 45 %; Figure 6). This suggests that there is no straightforward relationship between the concentration of aluminum (overall or that determined from pyridine adsorption) and ferrocene conversion. In other words, the n_{Si}/n_{Al} ratio does not seem to significantly influence the course of the acylation reaction.

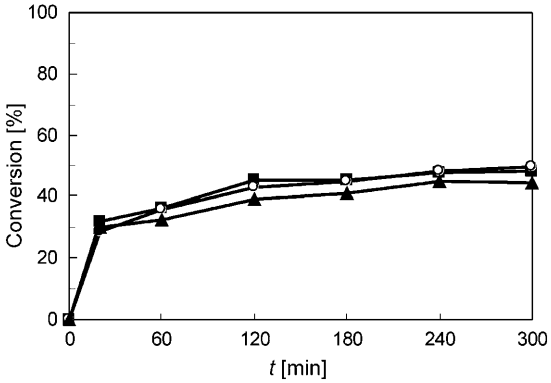

Figure 6. Acylation of ferrocene with 1-adamantoyl chloride: (■) AlKIT-5 (10), (○) AlKIT-5 (28), (▲) AlKIT-5 (44).

More importantly, however, the reaction affords exclusively (1-adamantoyl)ferrocene (i.e., the monoacylated product). This is rather surprising in view of the pore dimensions (5–6 nm) of the mesoporous catalysts, which are too large to sterically prevent twofold acylation that leads to 1,1′-bis(1-adamantoyl)ferrocene. In this case, mesoporous AlKIT-5 catalysts exert not only a higher selectivity but also higher yields when compared with the only heterogeneous catalyst reported to date, namely, bentonite-supported poly(trifluoromethanesulfosiloxane).[33] High yields of monoacylferrocenes were recently achieved also with alumina catalyst. However, trifluoroacetic anhydride had to be used to

activate carboxylic acids (both aliphatic and aromatic) to provide acylation activity.[34]

When cinnamoyl chloride was employed as the acylating agent, a substantial increase in ferrocene conversion over all AlKIT-5 catalysts was observed within the first 60 min of the reaction (Figure 7). Further prolongation of the reaction

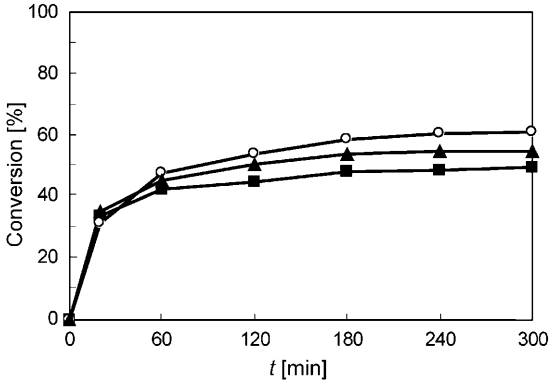

Figure 7. Acylation of ferrocene with cinnamoyl chloride: (■) AlKIT-5 (10), (○) AlKIT-5 (28), (▲) AlKIT-5 (44).

time led to only a slight increase in the ferrocene conversion, resulting in the order of conversions AlKIT-5 (10) 61% > AlKIT-5 (44) 55% > AlKIT-5 (28) 50%. Similarly to ferrocene acylation with 1-adamantoyl chloride, ferrocene conversions in the cinnamoylation reaction do not follow the order of acid site concentrations. However, the final ferrocene conversions are by about 5–12% higher compared with the acylation with 1-adamantoyl chloride. Such higher conversions can be attributed to the formation of a smaller product, which desorbs more easily from the catalysts.

In contrast to ferrocene acylation with 1-adamantoyl chloride, in which case the acylating agent was resistive to other reactions, cinnamoyl chloride was partly consumed by some competitive reactions. Despite these chemical complications, the cinnamoylation reaction also proved selective, thereby affording exlusively monocinnamoylferrocene.

Last but not least, acylation of ferrocene with benzoyl chloride, benzoic anhydride, and 2-chlorobenzoyl chloride was investigated (Figure 8) to better understand the differences in acylation activities of an acyl chloride and the corresponding anhydride and the effect of the electron-withdrawing chloride substituent at the benzene ring. In the acylation with benzoyl chloride, the conversions of ferrocene were similar with all catalysts (AlKIT-5 (28) and AlKIT-5 (10): 40%, AlKIT-5 (44): 35%). By contrast, ferrocene conversions in acylations with 2-chlorbenzoyl chloride were substantially lower and slightly decreased in the order AlKIT-5 (44) 20% > AlKIT-5 (28) 18% > AlKIT-5 (10) 14%. Such an observation is in agreement with the data published by Ma et al.,[12] who studied acylation of anisole with substituted benzoic acids. In the case of 2-chlorbenzoic acid, the conversion was 71%, whereas the conversion of benzoic acid was 76%.

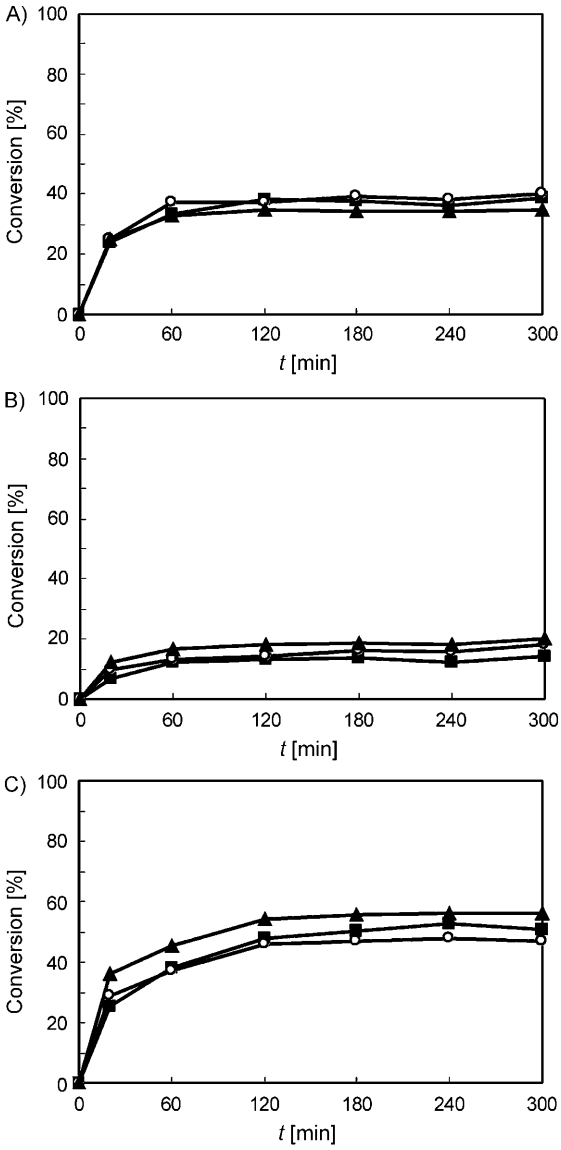

Figure 8. Acylation of ferrocene with A) benzoyl chloride, B) 2-chlorobenzoyl chloride, and C) benzoic anhydride. Catalysts: (■) AlKIT-5 (10), (○) AlKIT-5 (28), (▲) AlKIT-5 (44).

With benzoic anhydride as the acylating agent, the ferrocene conversions were approximately 10% higher than those achieved with benzoyl chloride, and decreased in the order AlKIT-5 (44) 56% > AlKIT-5 (10) 51% > AlKIT-5 (28) 47%. This again corresponds with the previous observation on toluene acylation, in which case acetic anhydride proved to be more reactive than acetyl chloride.[3] Bearing in mind that only one acyl moiety from the anhydride is utilized in the acylation reaction, the better ferrocene conversion is certainly not due to a higher concentration of the acyl moieties in the reaction mixture but more probably due to a different activation route of the acylating agent.

One of the most important issues connected with the application of AlKIT-5 in acylation of ferrocene is undoubtedly the possibility of catalyst recycling. This was tested in

four consecutive kinetic runs of ferrocene acylation with 1-adamantoyl chloride and the AlKIT-5 (10) catalyst, which was regenerated by simple heating to 500 °C in a stream of air for 2 h. Catalytic results presented in Figure 9 clearly indicate that the ferrocene conversion after each regeneration decreases only very slowly and remains higher than 40 % even after the fourth run. Very importantly, no changes in selectivity to the monocacylated products were noted during the repeated use of the catalyst.

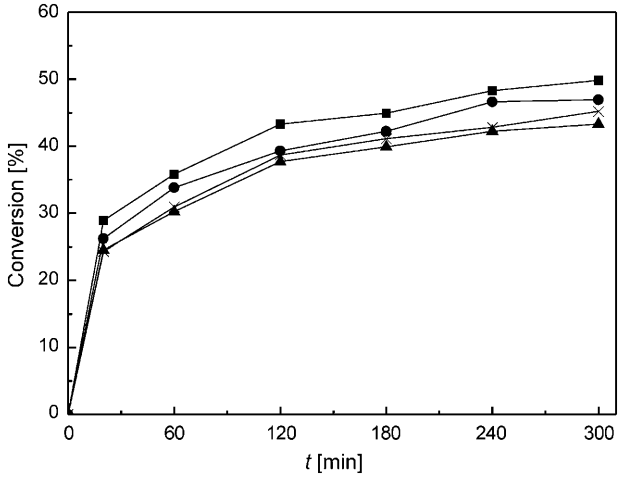

Figure 9. Acylation of ferrocene with 1-adamantoyl chloride over AlKIT-5 (10), run 1 (■), run 2 (●), run 3 (×), run 4 (▲).

Conclusion

The first demonstration of the high acylating ability of mesoporous catalysts in ferrocene acylation with bulky acylating agents is reported in this contribution. A series of Al-containing AlKIT-5 catalyst that differed by Al content was prepared by means of a direct synthesis method and was characterized by elemental analysis and mapping (EDS from electron microscopy), nitrogen adsorption isotherms, electron microscopy (HRSEM and HRTEM), powder X-ray diffraction, ^{27}Al MAS NMR spectroscopy, and pyridine adsorption/FTIR analysis. The analytical data indicated that the aluminum is evenly distributed within the parent KIT-5 structure; it is partly incorporated into the walls of the mesoporous molecular sieve AlKIT-5 and thus not available for catalytic reaction. Otherwise, however, the parent KIT-5 structure was found to be largely unaffected by the incorporation of Al ions, even in relatively high amounts.

The newly prepared materials were studied as catalysts for the acylation of ferrocene with bulky acylating agents. It was found that the reactions selectively afford monoacylferrocenes with the conversions of ferrocene decreasing in the following order of the acylating agents: cinnamoyl chloride > benzoic anhydride > 1-adamantoyl chloride > benzoyl chloride > 2-chlorobenzoyl chloride. For 1-adamantoyl chloride, cinnamoyl chloride, and benzoyl chloride, the highest ferrocene conversions were achieved with the AlKIT-5 catalyst that had a n_{Si}/n_{Al} ratio of 28, whereas, in the case of 2-chlorobenzoyl chloride and benzoic anhydride, the AlKIT-5 catalyst with a n_{Si}/n_{Al} ratio of 44 performed best. Still, however, the differences in ferrocene conversions with all tested acylating agents and all three AlKIT-5 catalyst were relatively minor (5–10 %), thereby indicating that the n_{Si}/n_{Al} ratio does not play any decisive role in determining the catalytic activity of the AlKIT-5 catalysts in this particular reaction.

The AlKIT-5 catalysts exhibit 100 % selectivity toward different acylferrocenes in ferrocene acylations. The origin of the high selectivity towards monoacylated products remains still uncertain. However, it can be tentatively sought in some deactivation of the primary monoacylated product towards the second acylation for steric and/or electronic reasons. Last but not least, the AlKIT-5 catalysts can be regenerated at least three times without any significant loss of the ferrocene conversion.

Acknowledgements

The authors thank the Grant Agency of the Academy of Sciences of the Czech Republic for financial support (project no. 104/07/0383). D.P. also acknowledges the support from the Grant Agency of the Czech Republic (203/08/H032). This work was further supported by the Ministry of Education, Culture, Sports, Science and Technology (MEXT) under the Strategic Program for Building an Asian Science and Technology Community Scheme and World Premier International Research Center (WPI) Initiative on Materials Nanoarchitectonics (MEXT, Japan), and is a part of the long-term research projects of the Faculty of Science, Charles University in Prague supported by the Ministry of Education of the Czech Republic (project no. MSM0021620857).

[1] R. A. Sheldon, H. Van Bekkum, *Fine Chemicals through Heterogeneous Catalysis*, Wiley-VCH, Weinheim, **2001**.
[2] G. Sartori, R. Maggi, *Chem. Rev.* **2006**, *106*, 1077.
[3] M. Bejblová, D. Procházková, J. Čejka, *ChemSusChem* **2009**, *2*, 486.
[4] L. Červený, K. Mikulcová, J. Čejka, *Appl. Catal. A* **2002**, *223*, 65.
[5] A. Vinu, J. Justus, C. Anand, D. P. Sawant, K. Ariga, T. Mori, P. Srinivasu, V. V. Balasubramanian, S. Velmathi, S. Alam, *Microporous Mesoporous Mater.* **2008**, *116*, 108.
[6] P. Botella, A. Corma, M. T. Navarro, F. Rey, G. Sastre, *J. Catal.* **2003**, *217*, 406.
[7] D. Procházková, M. Bejblová, J. Vlk, J. Čejka, *Top. Catal.* **2009**, *52*, 618.
[8] M. Bejblová, D. Procházková, J. Vlk, *Top. Catal.* **2009**, *52*, 178.
[9] D. P. Serrano, R. A. Garcia, D. Otero, *Appl. Catal. A* **2009**, *359*, 69.
[10] Y. Du, S. Liu, Y. Ji, Y. Zhang, F. Liu, Q. Gao, F.-S. Xiao, *Catal. Today* **2008**, *131*, 70.
[11] P. Srinivasu, S. Alam, V. V. Balasubramanian, S. Velmathi, D. P. Sawant, W. Böhlmann, S. P. Mirajkar, K. Ariga, S. B. Halligudi, A. Vinu, *Adv. Funct. Mater.* **2008**, *18*, 640.
[12] C. T. Kresge, M. E. Leonowicz, W. J. Roth, J. C. Vartuli, J. S. Beck, *Nature* **1992**, *359*, 710.
[13] A. Corma, *Chem. Rev.* **1997**, *97*, 2373.
[14] C. Márquez-Alvarez, N. Žilková N, J. Pérez-Pariente, J. Čejka, *Catal. Rev.* **2008**, *50*, 222.
[15] A. Sayari, *Chem. Mater.* **1996**, *8*, 1840.
[16] A. Taguchi, F. Schüth, *Microporous Mesoporous Mater.* **2005**, *77*, 1.

[17] V. V. Balasubramanian, P. Srinivasu, C. Anand, R. R. Pal, K. Ariga, S. Velmathi, S. Alam, A. Vinu, *Microporous Mesoporous Mater.* **2008**, *114*, 303.
[18] A. Vinu, M. Miyahara, K. Z. Hossain, M. Takahashi, V. V. Balasubramanian, T. Mori, K. Ariga, *J. Nanosci. Nanotechnol.* **2007**, *7*, 828.
[19] A. Vinu, M. Miyahara, V. Sivamurugan, T. Mori, K. Ariga, *J. Mater. Chem.* **2005**, *15*, 5122.
[20] See reference [11].
[21] See reference [17].
[22] M. Bejblová, S. I. Zones, J. Čejka, *Appl. Catal. A* **2007**, *327*, 255.
[23] *Ferrocenes: Ligands, Materials and Biomolecules* (Ed.: P. Štěpnička), Wiley, New York, **2008**.
[24] a) *Gmelin's Handbook of Inorganic Chemistry, New Supplement Series, Vol. 49, Organoiron Compounds, Part A: Ferrocene 2*, Springer, Berlin, **1977**; b) E. G. Perevalova, M. D. Reschetova, K. I. Grandberg, *Methods of Organometallic Chemistry, Ironorganic Compounds, Ferrocene*, Nauka Publishers, Moscow, **1983**, Chapter 3, pp. 40–128.
[25] Selected examples: a) RCOCl/[$Mo(CO)_6$]: H. Alper, S. M. Kempner, *J. Org. Chem.* **1973**, *38*, 2303; b) RCO_2H/ZnO: R. Wang, X. Hong, Z. Shan, *Tetrahedron Lett.* **2008**, *49*, 636; c) RCOCl/Zn: V. H. Purecha, N. S. Nandurkar, B. M. Bhanage, J. M. Nagarkar, *J. Chem. Res.* **2007**, 426.
[26] E. P. Barrett, J. G. Joyner, P. P. Halenda, *J. Am. Chem. Soc.* **1951**, *73*, 373.
[27] C. A. Emeis, *J. Catal.* **1993**, *141*, 347.
[28] J. Dědeček, N. Žilková, J. Čejka, *Microporous Mesoporous Mater.* **2001**, *44–45*, 299.
[29] B. Gil, S. I. Zones, S. J. Hwang, M. Bejblová, J. Čejka, *J. Phys. Chem. C* **2008**, *112*, 2997.
[30] M. Bejblová, J. Vlk, D. Procházková, H. Šiklová, J. Čejka, *Collect. Czech. Chem. Commun.* **2007**, *72*, 728.
[31] Acylferrocenes are highly versatile synthetic building blocks. For instance, they are readily converted to the corresponding optically pure secondary alcohols, which are precursors to various chiral phosphinoferrocene ligands. For representative references, see: a) J. Wright, L. Frambes, P. Reeves, *J. Organomet. Chem.* **1994**, *476*, 215. Besides, (2-chlorobenzoyl)ferrocene is an intermediate in a practical preparation of ferrocenecarboxylic acid; b) E. R. Biehl, P. C. Reeves, *Synthesis* **1973**, 360.
[32] Selected examples: a) J. Podlaha, P. Štěpnička, R. Gyepes, V. Mareček, A. Lhotský, M. Polášek, J. Kubišta, *Collect. Czech. Chem. Commun.* **1997**, *62*, 185; b) F. D. Popp, E. B. Moynahan, *J. Med. Chem.* **1970**, *13*, 1020; c) G. Mo, J. Ye, F.-S. Sheu, *Electrochem. Commun.* **2008**, *10*, 1490; d) Y. Yamaguchi, C. Kutal, *Macromolecules* **2000**, *33*, 1152; e) Y. Yamaguchi, B. J. Palmer, C. Kutal, T. Wakamatsu, D. B. Yang, *Macromolecules* **1998**, *31*, 5157; f) P. Kalenda, *Eur. Polym. J.* **1995**, *31*, 1099.
[33] R. J. Hu, B. G. Li, *Catal. Lett.* **2004**, *98*, 43.
[34] B. C. Ranu, U. Jana, A. Majee, *Green Chem.* **1999**, *1*, 33.

Received: January 26, 2010
Published online: June 2, 2010

